Solar sail orbital motion about asteriods and binary asteroid systems

Heiligers, Jeannette; Scheeres, Daniel J.

Publication date
2017

Document Version
Final published version

Published in
27th AAS/AIAA Space Flight Mechanics Meeting

AAS 17-377

SOLAR SAIL ORBITAL MOTION ABOUT ASTEROIDS AND BINARY ASTEROID SYSTEMS

Jeannette Heiligers[*] and Daniel J. Scheeres[†]

While SRP is often considered an undesirable effect, especially for missions to small bodies like asteroids and binary asteroid systems, this paper utilizes the SRP on a solar sail to generate artificial equilibrium points (AEPs) and displaced periodic orbits in these systems. While the solar sail dynamics for the single asteroid case are described using the Hill + SRP problem, those for the binary system are either described in the Hill four-body + SRP problem or the full bi-circular + SRP problem. The results for the single asteroid case include solar sail acceleration contours to remain stationary with respect to the asteroid on either the Sun-lit or dark side of the asteroid and either in or above its orbital plane. Using a combination of analytical and numerical methods, i.e., the Lindstedt-Poincaré method and a differential corrector, orbits around these AEPs can be found. By switching to the Hill four-body problem and employing a direct multiple shooting method, these orbits can be extended to a binary system where the effect of the smaller asteroid is an oscillatory motion around the orbits found for the single asteroid case. Finally, by switching to the bi-circular + SRP problem, AEPs can once again be obtained, though their location becomes time-dependent due to the changing direction of the Sun-vector. However, high above the binary system's orbital plane, the AEPs trace out a circular orbit that suggests the existence of so-called pole-sitter-like orbits. Using an analytical inverse method and a numerical differential corrector, the results indeed show families of solar sail periodic orbits above the binary system's orbital plane. Though all orbits, both in the single asteroid case and the binary system, are linearly unstable, they exist for near-term solar sail technology and for a simple steering law where the sail remains at a fixed attitude with respect to the Sun. These orbits therefore allow unique, geostationary-equivalent vantage points from where to monitor the asteroid(s) over extended periods of time.

INTRODUCTION

Solar sailing is a relatively new, but flight-proven form of low-thrust space propulsion [1, 2]. By exploiting the solar radiation pressure (SRP) on a large reflective membrane, solar sails can produce thrust

[*] Marie Curie Research Fellow, Delft University of Technology, Faculty of Aerospace Engineering, Kluyverweg 1, 2629 HS Delft, the Netherlands and University of Colorado, Department of Aerospace Engineering Sciences, Colorado Center for Astrodynamics Research, Boulder, CO 80309, USA. M.J.Heiligers@tudelft.nl

[†] A. Richard Seebass Endowed Chair Professor, University of Colorado Boulder, Department of Aerospace Engineering Sciences, Colorado Center for Astrodynamics Research, Boulder, CO 80309, USA. Scheeres@colorado.edu

without having to rely on an onboard supply of fuel [3, 4]. This unique capability allows solar sails to produce thrust over extended periods of time and build up large amounts of momentum over this mission time. Solar sails are therefore particularly suited for long-term and high-energy missions. Key mission concepts include: precessing an elliptical Earth-centered orbit for long residence times in the Earth's magnetotail (also known as the GeoSail mission concept) [5-8]; hovering along the Sun-Earth line sunward of the L_1-point for increased warning times for space weather events (also known as the GeoStorm mission concept) [9, 10]; and finally, of importance to the current paper, using the sail for close-up observations of a range of small bodies in a multiple near-Earth asteroid (NEA) rendezvous mission [11, 12]. The potential of solar sails for visiting NEAs will be demonstrated by NASA's proposed solar sail NEA Scout mission [13].

NASA's NEA Scout mission is only one of many examples that highlight the significant increase in interest in small body missions over recent years. This interest originates from a scientific perspective, because small bodies hold key information to the understanding of the origin and evolution of our solar system, but also from a planetary defense perspective as well as their potential as targets for future human space exploration activities. For close-up investigations of asteroids and other small bodies, a thorough understanding of the orbital motion around these bodies is key and abundant research in this field has demonstrated the challenge that solar radiation pressure poses to such small-body missions [14, 15]. However, instead of considering it an undesired effect, we exploit SRP in this paper in the form of solar sails to create entirely new orbital opportunities in the vicinity of asteroids.

The dynamics of a solar sail in close proximity to an asteroid have not yet been investigated in great detail. Previous work has mainly focused on terminator orbits [16] and the existence of hovering points at an asteroid [16-18]. These hovering points originate when adding a solar sail (or any low-thrust propulsion system [19, 20]) to a three-body system: any three-body system exhibits the well-known Lagrange points which can be extended to three-dimensional surfaces of artificial equilibrium points through a correct selection of sail acceleration and attitude. The purpose of the current paper is to complement these initial investigations with the existence of solar sail periodic orbits above the asteroid as well as extending the analyses to binary asteroid systems. In a binary asteroid system, surfaces of artificial equilibrium points can once again be obtained, though the topology of these surfaces changes over time, because the binary asteroids orbit each other while orbiting the Sun. Still, these AEPs can be used to generate a well-informed guess for solar sail periodic orbits above the binary asteroid's orbital plane. Such orbits, either above a single asteroid or a binary asteroid pair allow unique, geostationary-equivalent vantage points from where the asteroid or asteroid pair can be observed over extended periods of time.

For the analyses in this paper we assume a spherical, point mass asteroid, a perfectly reflecting solar sail and a circular heliocentric orbit of the asteroid/binary system about the Sun (at 1 astronomical unit (AU) for the binary system). Furthermore, for the binary system, we assume a zero inclination between the plane in which the two binaries orbit each other and their heliocentric orbital plane. Finally, to greatly simplify mission operations, all orbits are generated for a simple solar sail steering law that assumes a fixed attitude of the sail with respect to the Sun. Such an attitude can, in theory, be achieved passively through a correct offset between the sailcraft's center-of-mass and center-of-pressure.

DYNAMICAL MODELS

Depending on whether a single asteroid or a binary system is considered, either the framework of the Hill + SRP problem, the Hill four-body + SRP problem or the bi-circular + SRP problem is employed. Note that, for the single asteroid case, the Hill + SRP problem is required due to the very small mass of the asteroid with respect to the Sun and the expected close proximity of the spacecraft with respect to the asteroid [16].

The reference frames involved in all three dynamical systems are provided in Figure 1. When considering the Sun-asteroid Hill + SRP problem or Hill four-body + SRP problem, a rotating reference frame $R_1(\hat{\mathbf{x}},\hat{\mathbf{y}},\hat{\mathbf{z}})$ is employed that is centered at the (main) asteroid with the x-axis along the Sun-asteroid line, the z-axis perpendicular to the asteroid's heliocentric orbital plane and the y-axis completing the right-handed reference frame. When considering the binary asteroid bi-circular + SRP problem, again a rotating reference frame $R_2(\hat{\mathbf{x}},\hat{\mathbf{y}},\hat{\mathbf{z}})$ is employed, now with the x-axis connecting the two asteroids of the binary system, the z-axis perpendicular to the binary system's orbital plane and the y-axis completing the right-handed reference frame. The solar sail dynamics in either model can be written as [3, 16]:

$$\ddot{\mathbf{r}} + 2\boldsymbol{\Omega}\times\dot{\mathbf{r}} = \nabla U + \mathbf{a}_s \,. \tag{1}$$

In Eq. (1), $\mathbf{r}$ is the solar sail position vector in either $R_1(\hat{\mathbf{x}},\hat{\mathbf{y}},\hat{\mathbf{z}})$ or $R_2(\hat{\mathbf{x}},\hat{\mathbf{y}},\hat{\mathbf{z}})$, $\boldsymbol{\Omega}=\Omega\hat{\mathbf{z}}$ with Ω either the asteroid's orbit angular velocity around the Sun (Hill (four-body) + SRP problem) or the dimensionless angular velocity of the two asteroids around their common center-of-mass (bi-circular + SRP problem), U is the effective potential and $\mathbf{a}_s$ is the solar sail acceleration vector. Note that in the case of the bi-circular + SRP problem a set of canonical units is used whereby the sum of the two asteroids, the distance between them and $1/\Omega$ are taken as the unit of mass, length, and time, respectively. The definition of the effective potential is different for the three dynamical systems and is given as:

$$U=\begin{cases} \dfrac{\tilde{\mu}}{r}-\dfrac{1}{2}\Omega^2\left(z^2-3x^2\right) & \text{Hill + SRP problem} \\ \dfrac{\tilde{\mu}}{r}-\dfrac{1}{2}\Omega^2\left(z^2-3x^2\right)+\tilde{\mu}_3\left(\dfrac{1}{r_4}-\dfrac{\mathbf{r}\cdot\mathbf{r}_3}{r_3^3}\right) & \text{Hill four-body + SRP problem} \\ \left(\dfrac{1-\mu}{r_1}+\dfrac{\mu}{r_2}\right)+\dfrac{1}{2}\left(x^2+y^2\right)+\mu_3\left(\dfrac{1}{r_4}-\dfrac{\mathbf{r}\cdot\mathbf{r}_3}{r_3^3}\right) & \text{Bi-circular + SRP problem} \end{cases} \tag{2}$$

with $\tilde{\mu}$ the gravitational parameter of the single asteroid, $\tilde{\mu}_3$ the gravitational parameter of the perturbing, smaller asteroid in the binary system, $\mu=m_2/(m_1+m_2)$ (with m_1 and m_2 the masses of 'Asteroid 1' and 'Asteroid 2', respectively), $\mu_3=m_3/(m_1+m_2)$ (with m_3 the mass of the Sun) and r_1, r_2, r_3, and r_4 the magnitude of the vectors $\mathbf{r}_1=\mathbf{r}+\begin{bmatrix}\mu & 0 & 0\end{bmatrix}^T$, $\mathbf{r}_2=\mathbf{r}+\begin{bmatrix}\mu-1 & 0 & 0\end{bmatrix}^T$, $\mathbf{r}_3$ the position vector of the perturbing body, and $\mathbf{r}_4=\mathbf{r}_3-\mathbf{r}$, see Figure 1b. The vector $\mathbf{r}_3$ in either the Hill four-body or the bi-circular problem is defined as:

$$\mathbf{r}_3=\begin{cases} r_3\begin{bmatrix}\cos\omega t & \sin\omega t & 0\end{bmatrix}^T & \text{Hill four-body + SRP problem} \\ -r_3\hat{\mathbf{S}} & \text{Bi-circular + SRP problem} \end{cases}. \tag{3}$$

a)

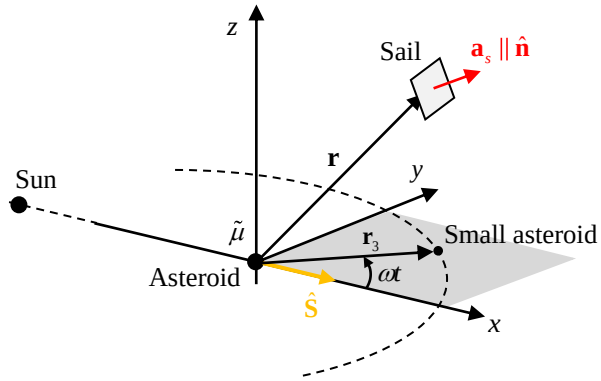

b)

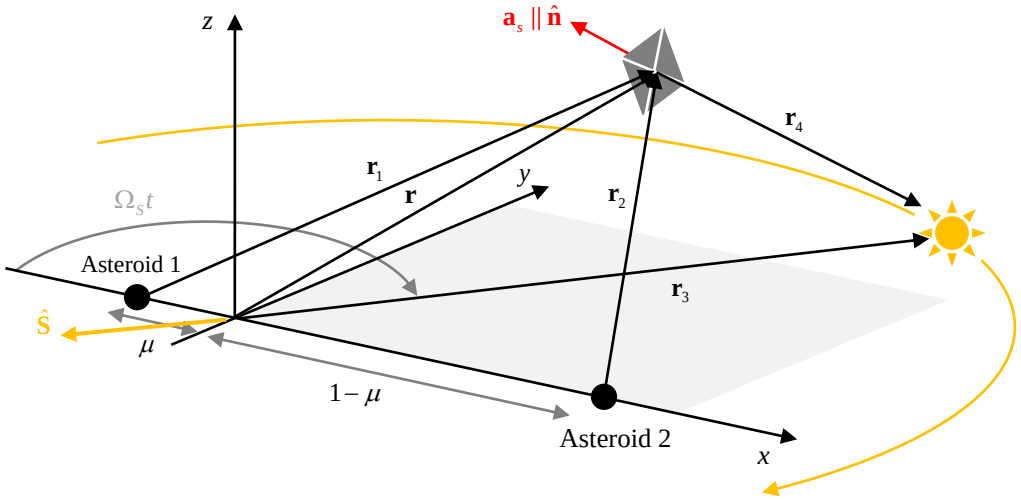

Figure 1a) Schematic of reference frame for Hill + SRP problem and Hill four-body + SRP problem. b) Schematic of bi-circular + SRP problem.

In the Hill four-body + SRP problem, r_3 equals the distance between the binary asteroids and ω is the angular rate of the binary system in the reference frame of Figure 1a, while in the bi-circular + SRP problem r_3 equals 1 AU and $\hat{\mathbf{S}}$ is the direction of Sunlight (see Figure 1b). Using the definitions in Figure 1, the unit vector $\hat{\mathbf{S}}$ can be defined as:

$$\hat{\mathbf{S}} = \begin{cases} \begin{bmatrix} 1 & 0 & 0 \end{bmatrix}^T & \text{Hill (four-body) + SRP problem} \\ \begin{bmatrix} \cos(\Omega_S t) & -\sin(\Omega_S t) & 0 \end{bmatrix}^T & \text{Bi-circular + SRP problem} \end{cases} \tag{4}$$

with Ω_S the dimensionless angular rate of the Sun around the binary system. Finally, the solar sail acceleration vector $\mathbf{a}_s = \begin{bmatrix} a_{s,x} & a_{s,y} & a_{s,z} \end{bmatrix}^T$, can be defined as:

$$\mathbf{a}_s = a_0 \left(\hat{\mathbf{S}} \cdot \hat{\mathbf{n}} \right)^2 \hat{\mathbf{n}} \tag{5}$$

with $\hat{\mathbf{n}}$ the normal vector to the sail membrane and a_0 the solar sail characteristic acceleration at the asteroid's or binary system's heliocentric distance (dimensionless for the case of the bi-circular + SRP problem). The characteristic acceleration is the acceleration produced by the sail when facing the Sun. Previous solar sail missions have achieved characteristic accelerations *at 1 AU* of $a_0 = 0.0059$ mm/s^2 (IKAROS (JAXA, 2010) [1]), $a_0 = 0.0178$ mm/s^2 (NanoSail-D2 (NASA, 2010) [2]), and $a_0 = 0.0652$ mm/s^2 (LightSail-1 (Planetary Society, 2015) [21]). A similar characteristic acceleration to that of LightSail-1 is expected for NASA's proposed NEA Scout mission, $a_0 = 0.0593$ mm/s^2 [13], while the previously proposed Sunjammer mission would have achieved a characteristic acceleration of $a_0 = 0.2153$ mm/s^2 [10]. The reduction in sail acceleration when pitching the sail away from the Sun is taken into account in Eq. (5) through the term $\left(\hat{\mathbf{S}}\cdot\hat{\mathbf{n}}\right)^2$. Finally, while the Sun is stationary in the Hill (four-body) + SRP problem, the Sun orbits around the binary system in the bi-circular + SRP problem and the smaller asteroid orbits around the main asteroid in the Hill four-body + SRP problem. As a result, the vectors $\mathbf{r}_3$ and $\hat{\mathbf{S}}$ change over time, which introduces a time dependency into the dynamics, causing the last two systems of equations in Eq. (1) to be non-autonomous.

ARTIFICIAL EQUILIBRIUM POINTS

When considering the Hill + SRP problem and the bi-circular + SRP problem, the approach in Reference [3] can be taken at hand to find artificial equilibrium points at either the single asteroid or within the binary system. When setting $\ddot{\mathbf{r}} = \dot{\mathbf{r}} = 0$ in Eq. (1), it becomes clear that the solar sail acceleration vector needs to counteract the gradient of the effective potential:

$$\nabla U = \mathbf{a}_s \,. \tag{6}$$

The required direction of the sail acceleration can be obtained by taking the cross product of both sides of Eq. (6) with $\hat{\mathbf{n}}$, resulting in

$$\nabla U \times \hat{\mathbf{n}} = 0 \,, \tag{7}$$

which gives

$$\hat{\mathbf{n}} = \frac{\nabla U}{\left|\nabla U\right|} \,. \tag{8}$$

Furthermore, the characteristic sail acceleration required to maintain a particular AEP can be obtained by taking the scalar product of Eq. (6) with $\hat{\mathbf{n}}$:

$$a_0 = \frac{\nabla U \cdot \hat{\mathbf{n}}}{\left(\hat{\mathbf{S}}\cdot\hat{\mathbf{n}}\right)^2} \,. \tag{9}$$

We first consider the AEPs at a single asteroid. The result in terms of solar sail acceleration contours required to transform a particular location in the (x,z)- or (x,y)-plane of the Hill frame into an AEP is provided in Figure 2, which are in agreement with the results found in Reference [16]. Note that the

distances on the horizontal and vertical axes are made dimensionless with respect to the Hill radius, $r_H = \sqrt[3]{\tilde{\mu}/\left(3\Omega^2\right)}$, whereas the sail acceleration is made dimensionless with respect to the asteroid's gravitational acceleration at the Hill radius. As a result, the figure can be applied to any asteroid. Finally, note that AEPs do not exist in the regions indicated with 'infeasible region' as they would require a solar sail acceleration component in the direction of the Sun, which the sail is unable to generate. The transition from 'feasible' to 'infeasible' is provided through the black (dotted) lines.

When considering AEPs in the binary system, we again note that due to the time dependency in the dynamics (through the vectors $\mathbf{r}_3$ and $\hat{\mathbf{S}}$) only *instantaneous* AEPs can be obtained. Furthermore, to generate results, a particular binary system, 1999 KW4, is assumed, which has served as a test case in previous studies, see for example Reference [22], and its characteristics are therefore well-documented, see Table 1. The red entries in Table 1 highlight the assumptions previously outlined in the introduction: that the orbit of 1999 KW4 is assumed to be a circular heliocentric orbit with a radius of 1 astronomical unit (AU) and that the Sun and binaries are assumed to orbit in the same plane.

The resulting solar sail dimensionless characteristic acceleration contours are provided in Figure 3 at time $t = 0$ (subplot a) and $t = 0.25\pi/\Omega_S$ (subplot b). Note that it takes the Sun just over one rotational period of the binary system to complete one revolution about the binary system, resulting in $\Omega_S =$ 0.99800. From comparing Figure 3a and Figure 3b it becomes clear that, as previously discussed, the contours change over time. Therefore, to maintain a single AEP, the attitude of the sail as well as the sail acceleration magnitude need to change over time. However, when plotting the contours on a plane that co-rotates with the Sun, see the gray (ρ, z)-plane in Figure 4a, the location of some of the contours remains nearly fixed. This is demonstrated in Figure 4b that shows how the contours for $a_0 = 10$ evolve over time when projected onto the (ρ, z)-plane of Figure 4a. Note that a value for the dimensionless characteristic acceleration of $a_0 = 10$ represents the expected performance of the previously proposed Sunjammer mission [10]. The colors indicate the time, $t \in [0, 2\pi/\Omega_S]$, but only the colors of the second half of the Sun's synodic period are visible as contours overlap due to the symmetry of the problem.

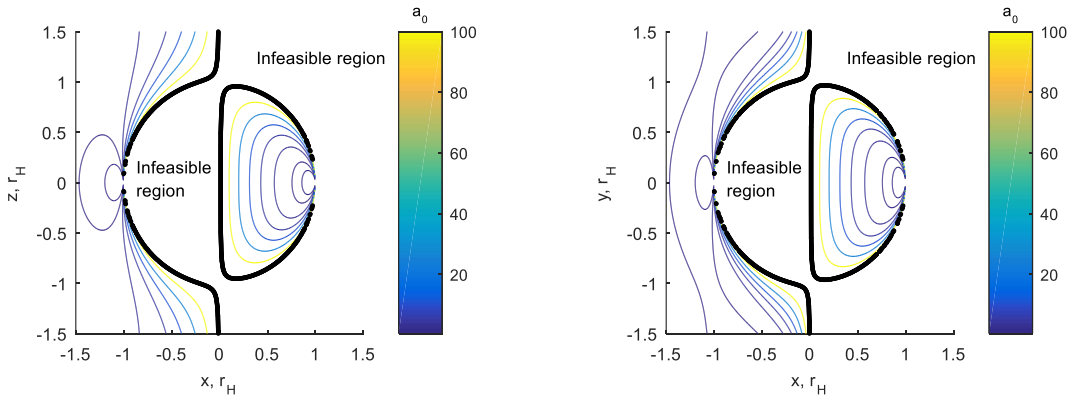

Figure 2 Solar sail acceleration contours to maintain an AEP in the Hill + SRP problem.

Table 1 Binary system 1999 KW4 parameters (partially from [22]).

Parameter	Value
Binary system	
Total mass of system	$m_1 + m_2 = 2.472 \times 10^{12}$ kg
Ratio of primary body and total mass	$\nu = 0.9457$
Mass ratio	$\mu = m_2 / (m_1 + m_2) = 1 - \nu = 0.0543$
Distance between bodies	$\lambda = 2.54$ km
Body radii (asteroid 1, asteroid 2)	0.75 km, 0.18 km
Rotational period of system	$P_{rot} = 17.458$ hr
Rotation rate in Hill reference frame	$\omega = 9.9774 \times 10^{-5}$ rad/s
Heliocentric orbit	
Semi-major axis	$a =$ ~~0.642 AU~~ 1 AU
Orbital period	$P_{orb} =$ ~~188 days~~ 365.25 days
Eccentricity	$e =$ ~~0.688~~ 0
Inclination	$i =$ ~~38.884 deg~~ 0 deg

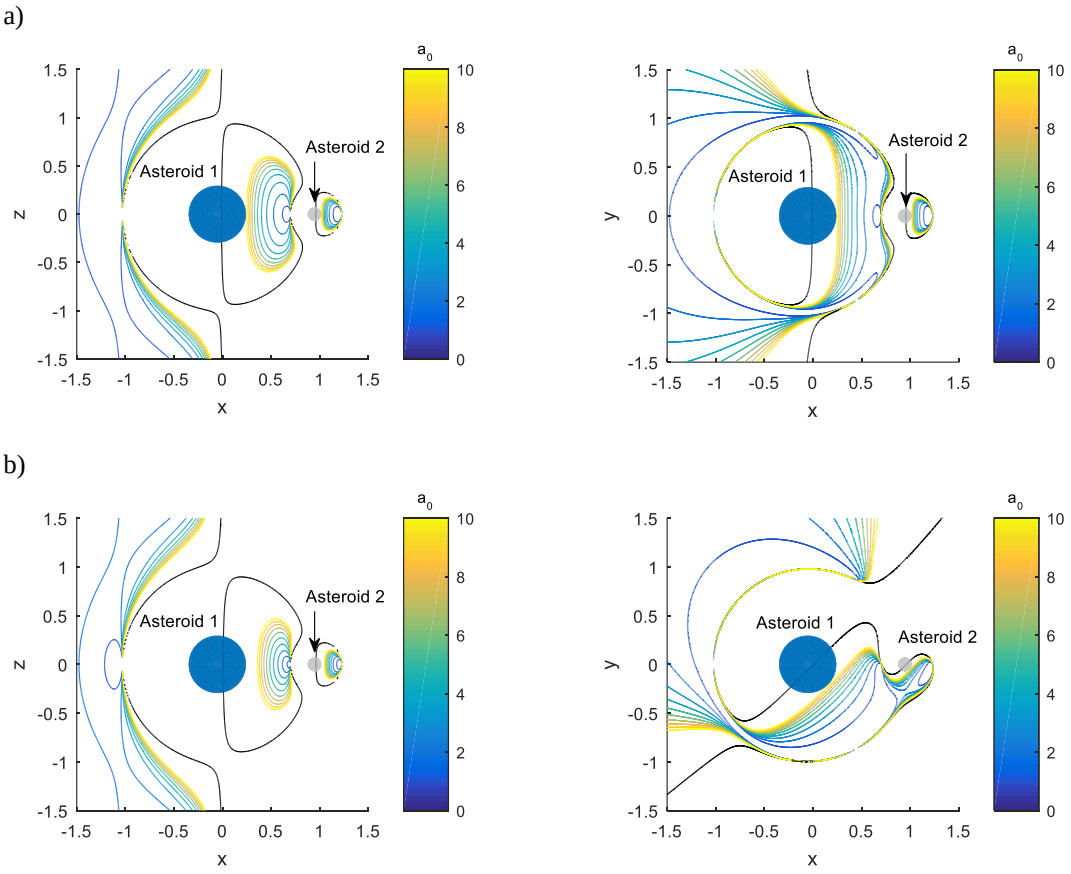

Figure 3 Solar sail acceleration contours to maintain an AEP in the bi-circular + SRP problem of binary system 1999 KW4. a) At time t = 0. b) At time $t = 0.25\pi/\Omega_s$.

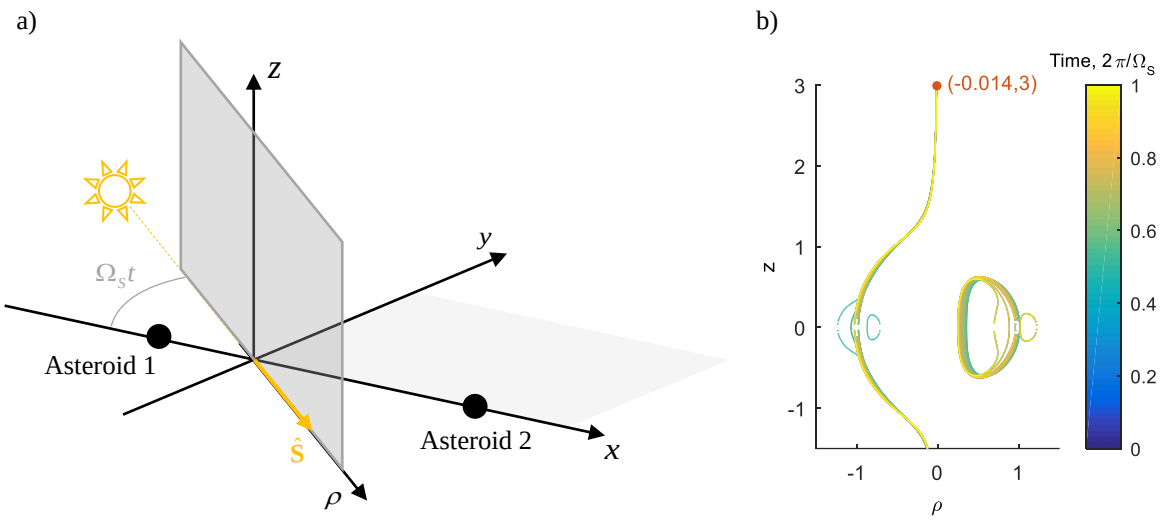

Figure 4 a) Schematic of (ρ,z)-plane co-rotating with the Sun. b) Evolution of AEP contours at 1999 KW4 for a_0 = 10 projected on the (ρ,z)-plane of subplot a).

SOLAR SAIL PERIODIC ORBITS IN THE SUN-ASTEROID HILL + SRP PROBLEM

Rather than hovering at a specific AEP, the solar sail can also be inserted into a periodic orbit around the AEP. The existence of such periodic orbits and the techniques required to obtain these periodic orbits have already been proven in the Sun-Earth circular restricted three-body problem [23, 24]. Adapting the technique to the dynamics of the Hill + SRP problem, an initial guess for such solar sail periodic orbits can be obtained through the following approach (with details in Reference [24]): first, we fix the attitude of the sail to the one of the AEP, see Eq. (8); we then approximate the equations of motion of the Hill + SRP dynamics in the neighborhood of the AEP by linearization and we expand the effective potential and solar sail acceleration terms to third order with a Taylor series; finally, we use the Lindstedt-Poincaré method to find the third-order solution to this approximated dynamical system.

Because the resulting solar sail periodic orbits are only approximations to the solutions of the full non-linear system, the orbit quickly diverges when integrating these initial conditions in Eq. (1). A differential correction scheme [10, 24, 25] is therefore employed to correct the initial conditions and find true solar sail periodic orbits in the full non-linear system.

Families of such periodic orbits around randomly selected AEPs are shown in Figure 5. The grey orbit indicates the third-order approximation of the orbit while the black orbits are families of orbits that exist in the full non-linear system and are parameterized by their z -amplitude. Note that all orbits exist for a constant sail attitude with respect to the Sun, prescribed by the required attitude of the AEP, see Eq. (8). While the top-left figure in Figure 5 holds for any asteroid, the other figures in Figure 5 provide details of the orbits at asteroid Vesta. For Vesta, the orbits for AEPs 1 and 3 can be obtained for a sail performance equal to that of The Planetary Society's LightSail-1 mission or NASA's NEA Scout mission [13], while the required sail performance for AEP 2 is much smaller, only one percent of that of LightSail-1 and NEA Scout.

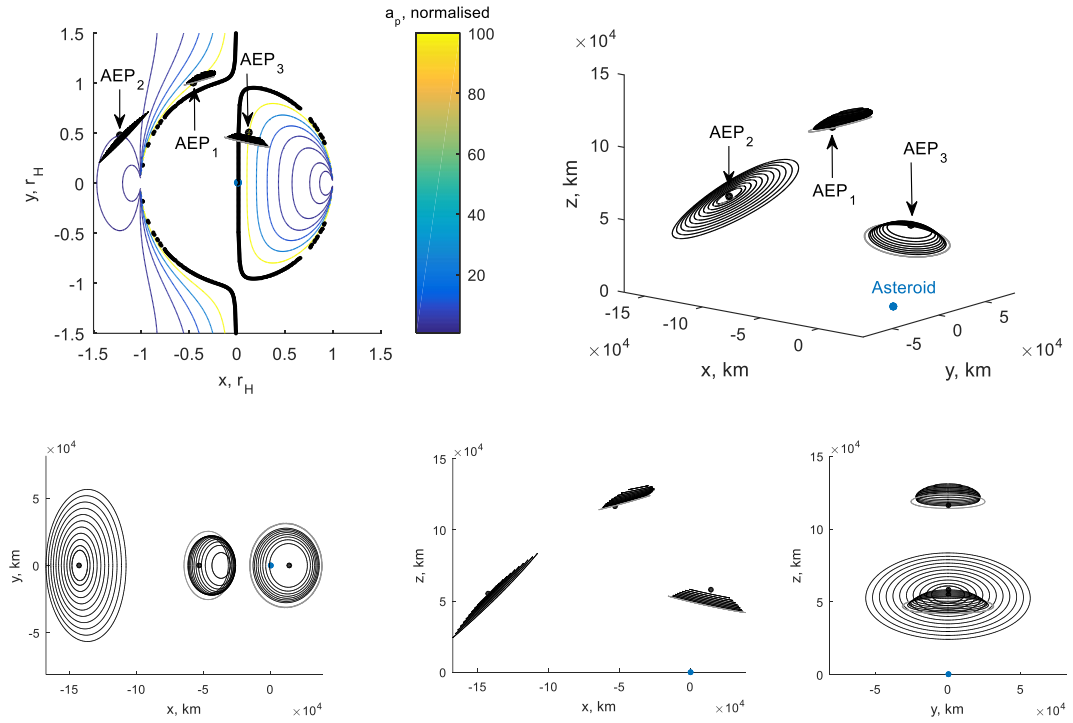

Figure 5 Solar sail periodic orbits around three AEPs at asteroid Vesta. Grey orbits are third body approximation whereas black orbits exist in the full non-linear system.

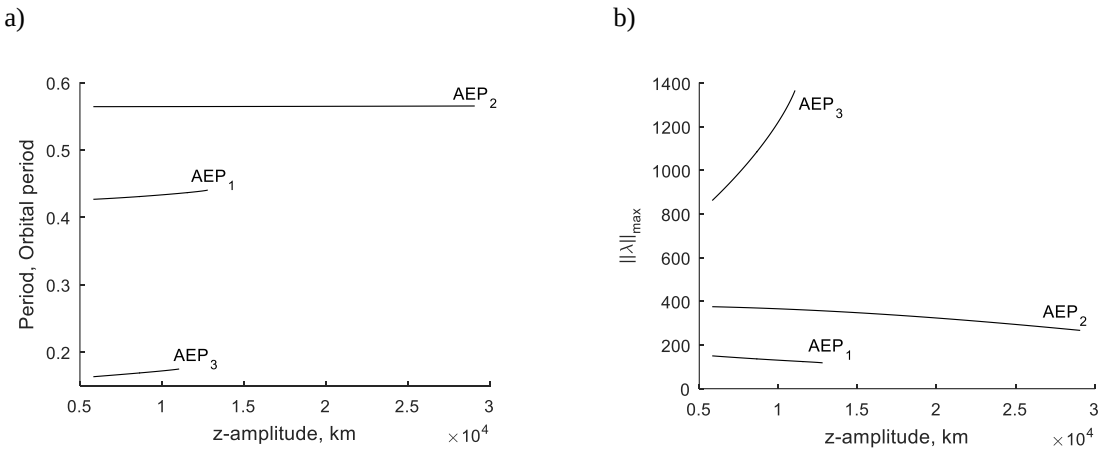

Figure 6 Details for solar sail periodic orbits in Figure 5. a) Orbital periods as a fraction of Vesta's orbital period. b) Linear stability.

The period of the orbits in Figure 5 are provided in Figure 6a, showing that the period is a significant fraction of the orbital period of the asteroid about the Sun. Furthermore, Figure 6b provides the linear stability of the orbits through the value of the largest eigenvalue, $\|\lambda\|_{\max}$, of the monodromy matrix (the state transition matrix evaluated after one full orbit). An orbit is stable if all six eigenvalues lie on the unit circle, i.e., $\|\lambda\|_{\max} = 1$. If the norm of any of the eigenvalues is larger than one, the orbit is unstable, with

larger norm values indicating greater instability. From Figure 6b it becomes clear that all orbits are unstable, but with increasing stability for AEPs 1 and 2 for increasing z-amplitudes, while the opposite holds true for AEP 3.

SOLAR SAIL PERIODIC ORBITS IN THE HILL FOUR-BODY + SRP PROBLEM

In order to assess the existence of solar sail periodic orbits around AEPs (similar to the ones shown in Figure 5) in a binary asteroid system, the Hill four-body + SRP problem is taken at hand to account for the perturbation from the smaller asteroid. Because the period of the solar sail orbits (see Figure 6a) and the period of the smaller asteroid around the main asteroid (the binary system's rotational period, see Table 1) are not commensurable, periodic orbits will no longer exist. However, by using techniques such as multiple shooting differential correction, orbits may still be found that remain close to the periodic orbit. To that end, the following approach is adopted: at first, the total mass of the binary system is assumed to be concentrated in a single asteroid, reducing the problem to the Hill + SRP problem for which solar sail periodic orbits exist similar to the ones shown in Figure 5. For binary system 1999 KW4 this results in the orbits provided in Figure 7. Subsequently, a continuation is started that gradually distributes the total mass over two asteroids, while at the same time gradually separating the two asteroids up to the total separation distance, λ ($\lambda =$ 2.54 km for 1999 KW4). Denoting the continuation parameter as $0 < \xi \leq (1-\nu)$, with ν the ratio of the main asteroid mass and the total system mass ($\nu =$ 0.9457 for 1999 KW4), the mass distribution during the continuation can be expressed as:

$$\begin{aligned} \tilde{\mu} &= (1-\xi)G(m_1+m_2) \\ \tilde{\mu}_3 &= \xi G(m_1+m_2) \end{aligned} . \tag{10}$$

At each step of the continuation, a multiple shooting differential correction (MSDC) scheme is employed to find the solar sail orbit that remains in close proximity of the periodic orbits in Figure 7. MSDC divides an initial guess of the trajectory into segments by defining patch points at appropriate locations. Subsequently, two differential correction 'levels' are applied to sequentially adjust the position of the patch points and the velocities at the patch points to find orbits that hold under the dynamics of the Hill four-body + SRP problem. Here, an accuracy on the mismatch in position at each patch point of 10^{-9} km is used and a mismatch in velocity of 10^{-9} km/s, *summed* over all patch points, is allowed. As initial guess for the very first step in the continuation (i.e., for a very small value for ξ), the black periodic orbits in Figure 7 are used, i.e., the orbits with the largest out-of-plane amplitude. The result obtained from this first step in the continuation is then used as initial guess to solve for a slightly larger value for ξ and this process is repeated until $\xi = (1-\nu)$. Further details on the MSDC scheme and its implementation can be found in References [26-28].

The result of the MSDC scheme is provided in Figure 8, which shows the original periodic orbit in the Hill + SRP problem (using a dashed grey line) and the perturbed orbits in the Hill four-body + SRP problem (in black). Here, the effect is evaluated for the duration of a single revolution of the original periodic orbit. The black lines clearly show the effect of the binary system's smaller asteroid as a short-duration oscillatory motion around the periodic orbits of the Hill + SRP problem.

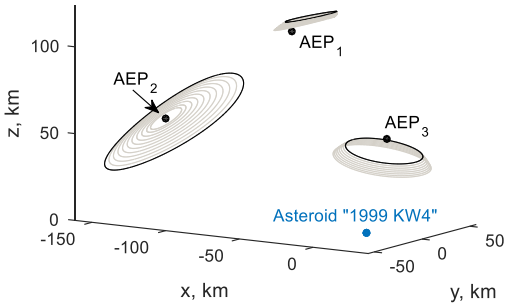

Figure 7 Solar sail periodic orbits around three AEPs at an asteroid with mass equal to the total mass of binary system 1999 KW4.

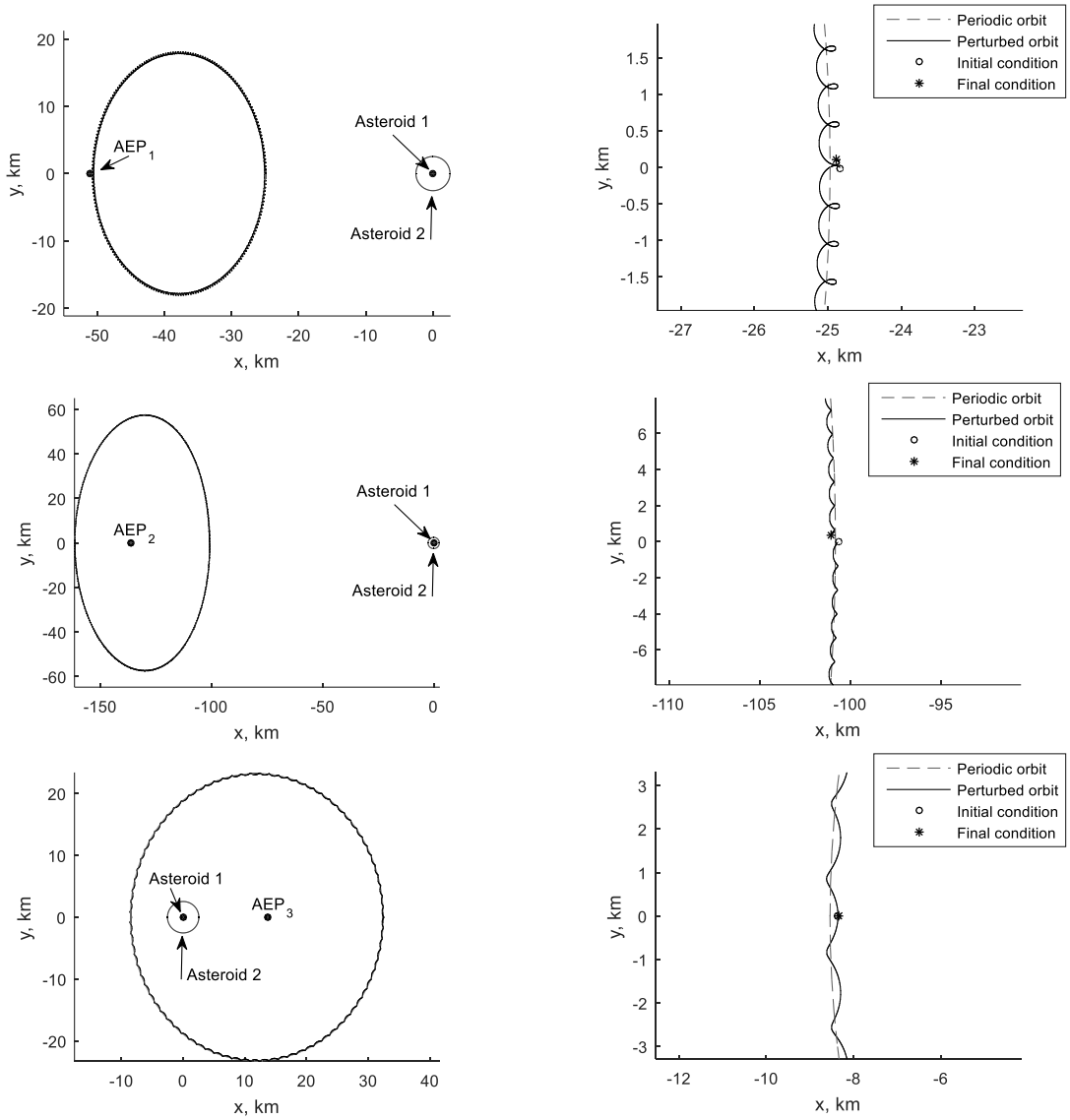

Figure 8 Oscillatory motion around the black periodic orbits in Figure 7 modelled in the 1999 KW4 Hill four-body + SRP dynamics. The right column provides details of the figures on the left.

SOLAR SAIL PERIODIC ORBITS IN THE BINARY SYSTEM BI-CIRCULAR + SRP PROBLEM

Instead of considering the smaller asteroid in the binary system as a perturbing body, which results in the quasi-periodic motion shown in Figure 8, true periodic orbits above a binary system can be found by considering the bi-circular + SRP problem. An initial guess for these orbits can be obtained from the information provided in Figure 4 as well as the techniques previously developed to obtain so-called pole-sitter orbits at Earth [29, 30] and other inner-Solar System planets [31]. The approach consists of assuming a particular shape for the orbit, inverting the equations of motion to obtain the required solar sail acceleration vector and using the resulting initial condition as an initial guess in a differential corrector scheme.

The assumed orbit is schematically shown in Figure 9. The orbit lies on a cone with half-angle θ around the z-axis, maintains a constant distance from the binary system's orbital plane and has an orbital period equal to the Sun's synodic period of $2\pi/\Omega_S$. As such, the position, velocity and acceleration in the orbit can be expressed as:

$$\mathbf{r}=\begin{bmatrix}x\\y\\z\end{bmatrix}=\begin{bmatrix}r\sin\theta\cos\Omega_S t\\-r\sin\theta\sin\Omega_S t\\r\cos\theta\end{bmatrix},\quad \dot{\mathbf{r}}=\begin{bmatrix}\dot{x}\\\dot{y}\\\dot{z}\end{bmatrix}=\begin{bmatrix}-\Omega_S r\sin\theta\sin\Omega_S t\\-\Omega_S r\sin\theta\cos\Omega_S t\\0\end{bmatrix},\quad \ddot{\mathbf{r}}=\begin{bmatrix}\ddot{x}\\\ddot{y}\\\ddot{z}\end{bmatrix}=\begin{bmatrix}-\Omega_S^2 r\sin\theta\cos\Omega_S t\\\Omega_S^2 r\sin\theta\sin\Omega_S t\\0\end{bmatrix}. \quad (11)$$

The initial condition (subscript '0') can then easily be obtained by substituting $t=0$ in Eq. (11):

$$\mathbf{r}_0=\begin{bmatrix}x_0\\y_0\\z_0\end{bmatrix}=\begin{bmatrix}r\sin\theta\\0\\r\cos\theta\end{bmatrix},\quad \dot{\mathbf{r}}_0=\begin{bmatrix}\dot{x}_0\\\dot{y}_0\\\dot{z}_0\end{bmatrix}=\begin{bmatrix}0\\-\Omega_S r\sin\theta\\0\end{bmatrix},\quad \ddot{\mathbf{r}}_0=\begin{bmatrix}\ddot{x}_0\\\ddot{y}_0\\\ddot{z}_0\end{bmatrix}=\begin{bmatrix}-\Omega_S^2 r\sin\theta\\0\\0\end{bmatrix}. \quad (12)$$

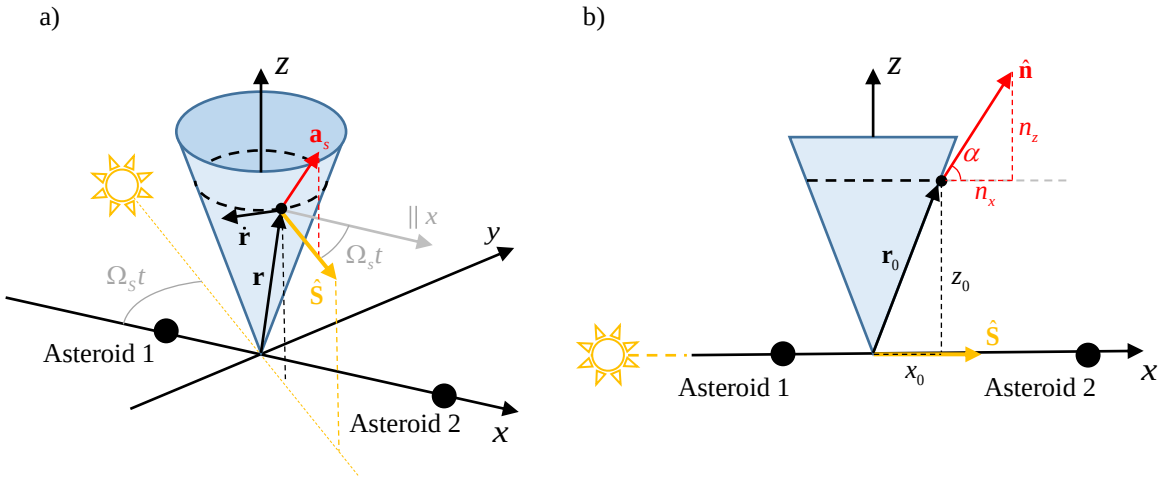

Figure 9 Schematic of assumed pole-sitter-like orbit. a) Generic case. b) Initial condition.

As a guess for r and θ, the results for the AEP indicated with a red round marker in Figure 4b are used:

$$\begin{aligned} r &= \sqrt{\rho^2 + z^2} = \sqrt{0.014^2 + 3^2} \\ \theta &= \tan^{-1}\left(\rho / z\right) = \tan^{-1}\left(0.014/3\right). \\ a_0 &= 10 \end{aligned} \tag{13}$$

With the evolution of the states preassigned, the equations of motion in Eq. (1) can be inverted to find *a guess* for the required solar sail normal vector at the initial time:

$$\begin{aligned} n_x\big|_0 &= \sqrt[3]{\frac{1}{a_0}\left(\ddot{x}_0 - 2\dot{y}_0 - x_0 + \frac{1-\mu}{r_1\big|_0^3}\left(\mu + x_0\right) + \frac{\mu}{r_2\big|_0^3}\left(-\left(1-\mu-x_0\right)\right) - \mu_3\left(\frac{1}{r_3^2} - \frac{x_0 + r_3}{r_4\big|_0^3}\right)\right)} \\ n_y\big|_0 &= 0 \\ n_z\big|_0 &= \frac{z_0}{a_0 n_x^2}\left(\frac{1-\mu}{r_1\big|_0^3} + \frac{\mu}{r_2\big|_0^3} + \frac{\mu_4}{r_4\big|_0^3}\right) \end{aligned}, \tag{14}$$

$$\hat{\mathbf{n}}_0 = \frac{\begin{bmatrix} n_x\big|_0 & 0 & n_z\big|_0 \end{bmatrix}^T}{\left\| \begin{bmatrix} n_x\big|_0 & 0 & n_z\big|_0 \end{bmatrix}^T \right\|}. \tag{15}$$

Finally, we assume that the attitude of the sail *with respect to the Sun co-rotating frame* of Figure 4a, $\hat{\mathbf{n}}_S$, *remains constant over time*. Because at time $t = 0$ it holds that $\hat{\mathbf{n}}_S = \hat{\mathbf{n}}_0$, the normal vector in the $R_2\left(\hat{\mathbf{x}}, \hat{\mathbf{y}}, \hat{\mathbf{z}}\right)$-frame (see Figure 1b) at any subsequent instance of time, t, can be obtained from

$$\hat{\mathbf{n}} = R_z\left(-\Omega_S t\right)\hat{\mathbf{n}}_S = R_z\left(-\Omega_S t\right)\hat{\mathbf{n}}_0 \tag{16}$$

with $R_z\left(-\Omega_S t\right)$ the rotation matrix around the z-axis over an angle $-\Omega_S t$.

Due to, among others, the assumption of a constant sail attitude with respect to the Sun, the initial condition in Eq. (12) will not lead to a periodic orbit when integrated in the dynamics of Eq. (1). However, it can serve as a good initial guess for a differential correction scheme similar to the one described in Reference [32] for solar sail periodic orbits in the non-autonomous solar sail Earth-Moon system. Note that this differential correction scheme includes a constraint to ensure that the period of the orbits equals $2\pi / \Omega_S$ in order for the orbital period and the period of the Sun around the binary system to be commensurable and thus for the orbits to be repeatable over time.The results are presented in Figure 10 to Figure 14.

Starting with the results in Figure 10, these show a family of pole-sitter-like orbits for $a_0 = 10$ that are parameterized by the sail cone angle, $\alpha = \cos^1\left(\hat{\mathbf{S}} \cdot \hat{\mathbf{n}}\right) = \tan^{-1}\left(n_z / n_x\right)$, see also Figure 9b. Figure 10a shows that the orbit can exist closer to the binary system's orbital plane for smaller cone angles (smaller out-of-plane components of the sail acceleration vector). However, for cone angles smaller than 73 deg, the differential corrector did not converge. Furthermore, the closer to the binary system (i.e., the smaller the cone angle), the more unstable the orbits become, see Figure 10b. More details for one of the orbits (with

$z = 10$ km) are provided in Figure 11, including the direction of the solar sail acceleration vector. Note that this sail attitude has been used to generate the results in Figure 12 to Figure 14.

Instead of parameterizing by the cone angle, the orbits can also be parameterized by the required solar sail characteristic acceleration. When assuming a sail attitude equal to that of the orbit in Figure 11, the family of orbits in Figure 12 can be obtained. Although the characteristic accelerations used to generate this family extend far beyond near-term sail technology, the figure shows that not much can be gained from very high-performing solar sails: to halve the distance to the binary asteroid's orbital plane (e.g., from 10 km to 5 km) the characteristic acceleration needs to be increased by an order of magnitude.

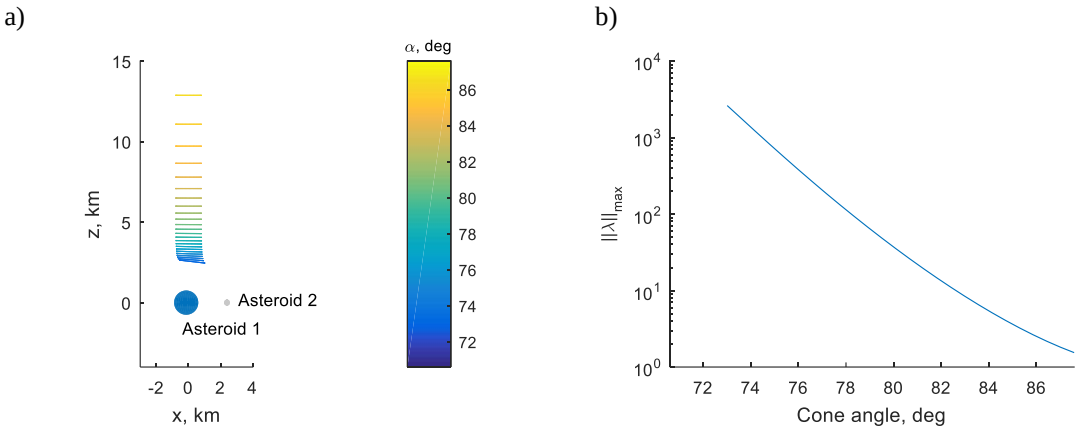

Figure 10 Family of pole-sitter-like orbits at 1999 KW4 for a_0 = 10, parameterized by the cone angle, α. a) Orbits. b) Linear stability.

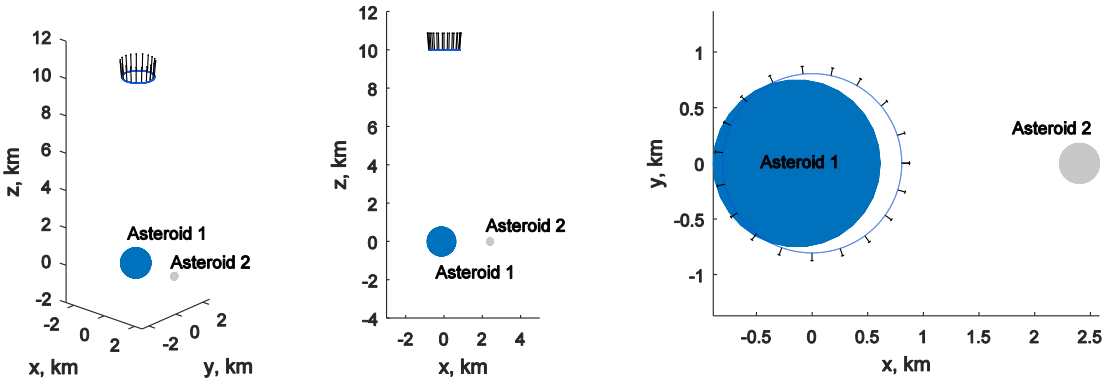

Figure 11 Details of pole-sitter-like orbit at z = 10 km. Arrows indicate the direction of the solar sail acceleration vector.

A third method of parameterization is shown in Figure 13, where families of periodic orbits for different heliocentric orbit radii of binary system 1999 KW4 are provided. Note that once again the sail attitude is fixed to that of the orbit in Figure 11 and that the sail performance is once again assumed to be $a_0 = 10$ *at 1 AU*. The figure shows that the pole-sitter-like orbit moves farther away for larger heliocentric orbit radii, which is caused by the decrease in solar radiation pressure. An additional effect of an increased heliocentric orbit radius is a decrease in the orbit period because the Sun's synodic period decreases and approaches the binary system's rotational period. This effect is demonstrated in Figure 13b.

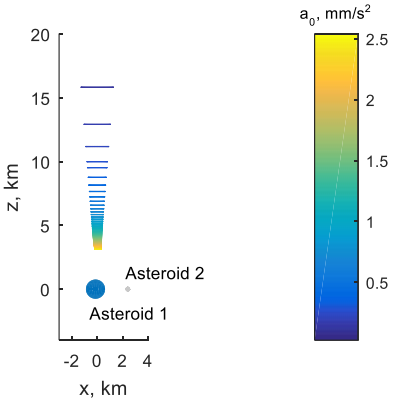

Figure 12 Family of pole-sitter-like orbits at 1999 KW4 for a sail attitude equal to that of the orbit in Figure 11, parameterized by the characteristic acceleration, a_0.

a) b)

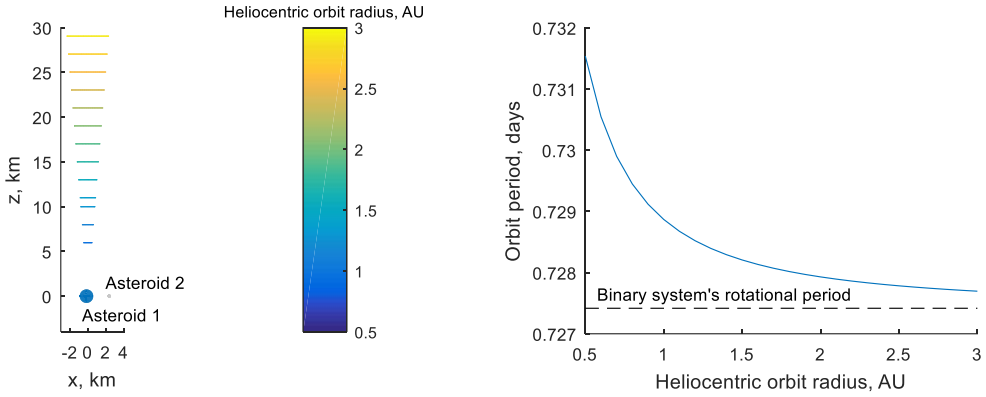

Figure 13 Family of pole-sitter-like orbits at 1999 KW4 for $a_0 = 10$ and a sail attitude equal to that of the orbit in Figure 11, parameterized by the binary system's heliocentric orbit radius. a) Orbits. b) Orbital period.

Finally, in Figure 14 the effect of the mass distribution between the two asteroids is demonstrated. The figure shows a family of pole-sitter-like orbits for a sail attitude equal to that of the orbit in Figure 11, for $a_0 = 10$, and for a heliocentric orbit radius of 1 AU. While the actual mass distribution for binary system

1999 KW4 is $\nu = 0.9457$, Figure 14 shows the effect in case this value is not correct and takes it to the extreme where the mass distribution is inverted ('Asteroid 2' is more massive than 'Asteroid 1'). For a clear presentation of the results, the reference frame is now centered at the *geometrical* center of the binary system. Furthermore, the sizes of the asteroids in Figure 14 are not accurate as these sizes will most likely change for different values for ν. What this reference frame clearly shows is how the orbit moves from hovering above 'Asteroid 1' (for $\nu > 0.5$) to hovering above 'Asteroid 2' (for $\nu < 0.5$).

The results throughout Figure 10 to Figure 14 have shown that pole-sitter-like orbits exist for a range of sail attitudes and sail acceleration magnitudes and that the existence and shape of the pole-sitter-like orbits do not break down for heliocentric orbit radii or mass distributions different from those for binary asteroid system 1999 KW4. However, other system parameters that have been neglected so far (see the red entries in Table 1) such as the eccentricity of the heliocentric orbit, the inclination of the orbit with respect to the binary system's orbital plane as well as other effects such as a non-spherical shape of one (or both) of the asteroids may effect these pole-sitter-like orbits. These effects will therefore be investigated in future work.

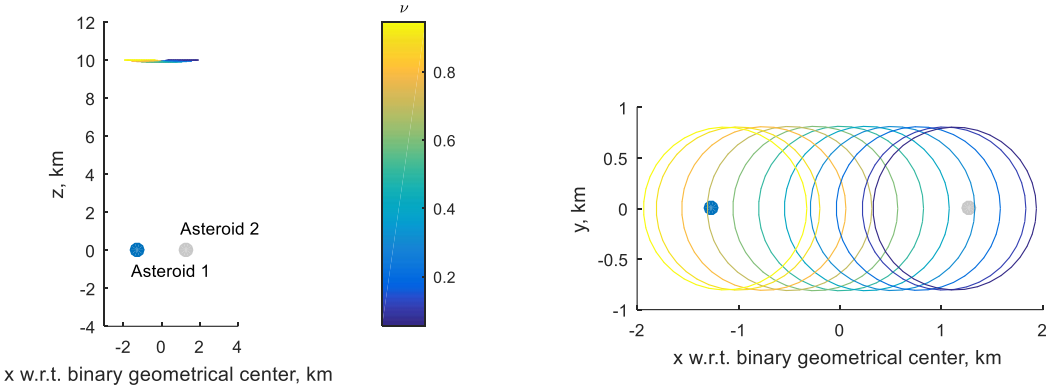

Figure 14 Family of pole-sitter-like orbits at 1999 KW4 for a_0 = 10 and a sail attitude equal to that of the orbit in Figure 11, parameterized by the mass distribution between the two asteroids ν. Note that the frame's origin is centered at the binary system's *geometrical* center.

CONCLUSIONS

This paper has demonstrated the existence of solar sail artificial equilibrium points (AEPs) at asteroids and binary asteroid systems as well as solar sail periodic orbits above their orbital planes. For the single asteroid case, solar sail acceleration contours have been obtained in the Hill + SRP problem that allow the sailcraft to remain stationary with respect to the asteroid on either the Sun-lit or dark side of the asteroid and either in or above its orbital plane. Furthermore, families of solar sail periodic orbits around these AEPs have been generated, where each orbit within a family only differs in its out-of-plane amplitude. These orbits have been found for near-term sail technology and for periods equal to a significant fraction of the asteroid's heliocentric orbital period. When taking asteroid Vesta as a test case, sailcraft-asteroid

distances in the order of 10^4 km can be achieved. When adding a fourth body to the Hill + SRP dynamics to simulate a binary asteroid system, the smaller asteroid creates a small oscillatory motion around the displaced orbits, causing quasi-periodic motion. When modelling the binary system in the bi-circular + SRP problem, AEPs and truly periodic orbits can once again be obtained, though the location of the AEPs becomes time-dependent due to the changing direction of the Sun-vector. Taking binary system 1999 KW4 as a test case, families of pole-sitter-like orbits above the binary orbital plane have been generated that can be parameterized, for example, by the required sail characteristic acceleration, the sail attitude, the heliocentric distance or even the mass distribution within the binary system. For large ranges in the values for these parameters, the existence of pole-sitter-like orbits above the binary system has been demonstrated at sailcraft-binary distances in the order of 10 km for near-term sail technology. While all orbits presented (both for the single asteroid case and the binary system) are linearly unstable, they do allow a unique vantage point from where to observe the asteroid or asteroid pair. Furthermore, all orbits exist for a simple solar sail steering law where the attitude is fixed with respect to the Sun, which greatly simplifies mission operations. Finally, with the solar sail as a propellant-less propulsion system, where the mission duration is only constrained by the lifetime of the sail membrane in the space environment, these orbits can theoretically be maintained indefinitely.

ACKNOWLEDGMENTS

Jeannette Heiligers would like to acknowledge support from the Marie Skłodowska-Curie Individual Fellowship 658645 - S4ILS: Solar Sailing for Space Situational Awareness in the Lunar System.

REFERENCES

1. Tsuda, Y., Mori, O., Funase, R., Sawada, H., Yamamoto, T., Saiki, T., Endo, T., Yonekura, K., Hoshino, H., and Kawahuchi, J., "Achievement of IKAROS - Japanese deep space solar sail demonstration mission," *Acta Astronautica*; Vol. 82, 2013, pp. 183-188. doi: 10.1016/j.actaastro.2012.03.032
2. Johnson, L., Whorton, M., Heaton, A., Pinson, R., Laue, G., and Adams, C., "NanoSail-D: A Solar Sail Demonstration Mission," *Acta Astronautica*; Vol. 68, 2011, pp. 571-575. doi: 10.1016/j.actaastro.2010.02.008
3. McInnes, C.R., "Solar Sailing: Technology, Dynamics and Mission Applications," *Springer-Praxis Books in Astronautical Engineering*, Springer-Verlag, Berlin, 1999.
4. Vulpetti, G., Johnson, L., and Matloff, G.L., "Solar Sails A Novel Approach to Interplanetary Travel, 2nd Edition," *Springer-Praxis Books in Space Exploration*, 2nd ed., Springer Science+Business Media, New York, 2015.
5. Macdonald, M., McInnes, C., Alexander, D., and Sandman, A., "GeoSail: Exploring the Magnetosphere Using a Low-cost Solar Sail," *Acta Astronautica*; Vol. 59, 2006, pp. 757-767. doi: 10.1016/j.actaastro.2005.07.023
6. Macdonald, M. and McInnes, C., "Solar Sail Science Mission Applications and Advancement," *Advances in Space Research*; Vol. 48, No. 11, 2011, pp. 1702-1716. doi: 10.1016/j.asr.2011.03.018
7. McInnes, C.R., Macdonald, M., Angelopolous, V., and Alexander, D., "GEOSAIL: Exploring the Geomagnetic Tail Using a Small Solar Sail," *Journal of Spacecraft and Rockets*; Vol. 38, No. 4, 2001, pp. 622-629. doi: 10.2514/2.3727

8. Macdonald, M., Hughes, G., McInnes, C., A, L., Falkner, P., and Atzei, A., "GeoSail: An Elegant Solar Sail Demonstration Mission," *Journal of Spacecraft and Rockets*; Vol. 44, No. 4, 2007, pp. 784-796. doi: 10.2514/1.22867
9. West, J.L., "The GeoStorm Warning Mission: Enhanced Opportunities Based on New Technology," *14th AAS/AIAA Spaceflight Mechanics Conference*, AAS-04-102, Maui, Hawaii, 2004.
10. Heiligers, J., Diedrich, B., Derbes, B., and McInnes, C.R., "Sunjammer: Preliminary End-to-End Mission Design," *2014 AIAA/AAS Astrodynamics Specialist Conference*, San Diego, CA, USA, 2014.
11. Dachwald, B., Boehnhardt, H., Broj, U., Geppert, U.R.M.E., Grundmann, J.-T., Seboldt, W., Seefeldt, P., Spietz, P., Johnson, L., Kührt, E., Mottola, S., Macdonald, M., McInnes, C.R., Vasile, M., and Reinhard, R., *Gossamer Roadmap Technology Reference Study for a Multiple NEO Rendezvous Mission*, in *Advances in Solar Sailing*, M. Macdonald, Editor. 2014, Springer Berlin Heidelberg: Berlin, Heidelberg. p. 211-226.
12. Peloni, A., Ceriotti, M., and Dachwald, B., "Solar-Sail Trajectory Design for a Multiple Near-Earth-Asteroid Rendezvous Mission," *Journal of Guidance, Control, and Dynamics*; Vol., 2016, pp. 0-0. doi: 10.2514/1.G000470
13. McNutt, L., Johnson, L., Clardy, D., Castillo-Rogez, J., Frick, A., and Jones, L., "Near-Earth Asteroid Scout," *AIAA SPACE 2014 Conference and Exposition*, American Institute of Aeronautics and Astronautics, San Diego, CA, 2014.
14. Scheeres, D.J., "Orbital Motion in Strongly Perturbed Environments - Applications to Asteroid, Comet and Planetary Satellite Orbiters," Springer-Praxis Books in Astronautical Engineering, Berlin Heidelberg, 2012.
15. Scheeres, D.J., "Orbit Mechanics About Asteroids and Comets," *Journal of Guidance, Control, and Dynamics*; Vol. 35, No. 3, 2012, pp. 987-997. doi: 10.2514/1.57247
16. Morrow, E., Scheeres, D.J., and Lubin, D., "Solar Sail Operations at Asteroids," *Journal of Spacecraft and Rockets*; Vol. 38, No. 2, 2001, pp. 279-286. doi: 10.2514/2.3682
17. Gong, S. and Li, J., "Equilibria near Asteroids for Solar Sails with Reflection Control Devices," *Astrophysics and Space Science*; Vol. 355:0, 2015. doi: 10.1007/s10509-014-2165-7
18. Williams, T. and Abate, M., "Capabilities of Furlable Solar Sails for Asteroid Proximity Operations," *Journal of Spacecraft and Rockets*; Vol. 46, No. 5, 2009, pp. 967-975. doi: 10.2514/1.30355
19. McKay, R.J., Macdonald, M., Biggs, J., and McInnes, C., "Survey of Highly Non-Keplerian Orbits with Low-Thrust Propulsion," *Journal of Guidance, Control, and Dynamics*; Vol. 34, No. 3, 2011. doi: 10.2514/1.52133
20. Morimoto, M., Yamakawa, H., and Uesugi, K., "Periodic Orbits with Low-Thrust Propulsion in the Restricted Three-Body Problem," *Journal of Guidance, Control, and Dynamics*; Vol. 29, No. 5, 2006, pp. 1131-1139. doi: 10.2514/1.19079
21. Biddy, C. and Svitek, T., "LightSail-1 Solar Sail Design and Qualification," *Proceedings of the 41st Aerospace Mechanisms Symposium*, Pasadena, CA, 2012.
22. Bellerose, J. and Scheeres, D., "Restricted Full Three-Body Problem: Application to Binary System 1999 KW4," *Journal of Guidance, Control, and Dynamics*; Vol. 31, No. 1, 2008, pp. 162-171. doi: 10.2514/1.30937
23. Baoyin, H. and McInnes, C., "Solar Sail Halo Orbits at the Sun-Earth Artificial L1-point," *Celestial Mechanics and Dynamical Astronomy*; Vol. 94, 2006, pp. 155-171. doi: 10.1007/s10569-005-4626-3
24. Waters, T.J. and McInnes, C.R., "Periodic Orbits Above the Ecliptic in the Solar-Sail Restricted Three-Body Problem," *Journal of Guidance, Control, and Dynamics*; Vol. 30, No. 3, 2007, pp. 687-693. doi: 10.2514/1.26232
25. Howell, K.C., "Three-Dimensional, Periodic, 'Halo' Orbits," *Celestial Mechanics and Dynamical Astronomy*; Vol. 32, 1983, pp. 53-71. doi: 10.1007/BF01358403
26. Parker, J.S. and Anderson, R.L., "Low-Energy Lunar Trajectory Design," *Deep Space Communications and Navigation Series*, Jet Propulsion Laboratory, Pasadena, California, USA, 2013.
27. Howell, K.C. and Pernicka, H.J., "Numerical Determination of Lissajous Trajectories in the Restricted Three-Body Problem," *Celestial Mechanics*; Vol. 41, 1988, pp. 107-124

28. Marchand, B.G., Howell, K.C., and Wilson, R.S., "Improved Corrections Process for Constrained Trajectory Design in the n-Body Problem," *Journal of Spacecraft and Rockets*; Vol. 44, No. 4, 2007, pp. 884-897
29. Heiligers, J., Ceriotti, M., McInnes, C.R., and Biggs, J.D., "Mission Analysis and Systems Design of a Near-Term and Far-Term Pole-Sitter Mission," *Acta Astronautica*; Vol. 94, No. 1, 2014. doi: 10.1016/j.actaastro.2012.12.015
30. Ceriotti, M., Heiligers, J., and McInnes, C.R., "Trajectory and Spacecraft Design for a Pole-Sitter Mission," *Journal of Spacecraft and Rockets*; Vol. 51, No. 1, 2014, pp. 311-326. doi: 10.2514/1.A32477
31. Walmsley, M., Heiligers, J., Ceriotti, M., and McInnes, C., "Optimal Trajectories for Planetary Pole-Sitter Missions," *Journal of Guidance, Control, and Dynamics, Under Review*; Vol., 2016
32. Heiligers, J., Macdonald, M., and Parker, J.S., "Extension of Earth-Moon Libration Point Orbits with Solar Sail Propulsion," *Astrophysics and Space Sciences, In Press*; Vol. 361 : 241, 2016. doi: 10.1007/s10509-016-2783-3